

# Longitudinal stability and control augmentation with robustness and handling qualities requirements using the two degree of freedom controller

Francisco J. Triveno Vargas<sup>1</sup> · Fernando J. de Oliveira Moreira<sup>1</sup> · Pedro Paglione<sup>2</sup>

Received: 30 September 2013 / Accepted: 22 September 2015 / Published online: 9 October 2015  
© The Brazilian Society of Mechanical Sciences and Engineering 2015

**Abstract** This paper presents a practical design of longitudinal stability and control augmentation system (SCAS) using a two degree of freedom (TDOF) controller. It is based on the linear quadratic regulator (LQR) technique in the frequency domain, via spectral factorization. The controller exhibits robustness to plant uncertainties, related with variation due to different operation conditions, and incorporates various aircraft handling qualities (HQ) requirements to comply with certification authority's requests. The project results in an unique set of fixed gain TDOF controller for a plant dynamics which changes with a  $V_{CAS} \times x_{cg}$  envelope. The project is done aiming at the industrial implementation of TDOF controller in fly-by-wire aircrafts.

**Keywords** Stability control augmentation · Two degree of freedom · Spectral factorization · Handling qualities · Fly-by-wire

## List of symbols

$x_{cg}$  Center of gravity (%)  
 $\omega_n$  Natural frequency (rad/s)

$\phi$	Roll angle (rad)
$\theta$	Pitch angle (rad)
$\psi$	Yaw angle (rad)
$p$	Roll rate (rad/s)
$q$	Pitch rate (rad/s)
$r$	Yaw rate (rad/s)
$V_{CAS}$	Calibrated airspeed (knots)
$V_{TAS}$	True airspeed (m/s)
$\mathbf{V}$	Velocity vector (m/s)
$\alpha$	Attack angle (rad)
$\beta$	Sideslip angle (rad)
$\gamma$	Flight path angle (rad)
$\delta_e$	Elevator angle (rad)
$\tau$	Delay of sensor (ms)
$\tau_p$	Phase delay criteria (s)
$\zeta$	Damping factor (dimensionless)
$j$	Imaginary number (dimensionless)
$\rho, \sigma$	Weighting factors (dimensionless)
$\kappa$	Steady state gain (dimensionless)
$\hat{q}(s), h(s), k(s)$	Controller gains (dimensionless)
$x_s$	$x$ axis stability coordinate system (dimensionless)
$x_\omega$	$x$ axis wind coordinate system (dimensionless)
$x_b$	$x$ axis body coordinate system (dimensionless)

Technical Editor: Glauco A. de P. Caurin.

✉ Francisco J. Triveno Vargas  
francisco.vargas@embraer.com.br

Fernando J. de Oliveira Moreira  
fernando.moreira@embraer.com.br

Pedro Paglione  
paglione@ita.br

<sup>1</sup> EMBRAER S.A, São Jose dos Campos, Brazil

<sup>2</sup> Departamento de Mecânica de Voo, Instituto Tecnológico de Aeronáutica (ITA), São Jose dos Campos, Brazil

## 1 Introduction

The traditional design of flight control laws typically uses nonlinear techniques to make the aircraft insensitive to changes in flight conditions and aircraft configuration (e.g., mass, center of gravity ( $x_{cg}$ ), airspeed, altitude, flap position, etc.). The inability to take into account these changes

in the design can result in stability degradation over the flight envelope. A dynamic mode that is stable and adequately damped in one flight condition may become either lightly damped or even unstable in another one. In commercial aircraft, such as stability degradation, can cause some discomfort to passengers and, even worst, reduce the pilot capability to handling the aircraft. Therefore, improving stability is an additional target to flight control laws.

Feedback control also provides benefits in terms of aircraft weight reduction, aerodynamic efficiency and optimization of fuel consumption. Such benefits are shown in [1], with the use of fly-by-wire control laws of a new transport aircraft. Such control laws are known in aeronautics as stability augmentation systems (SAS), if they affect damping and natural frequencies to improve the aircraft transient response, or, as control augmentation systems (CAS), if the purpose is to give the pilot more precise control, for instance the sideslip  $\beta$  limiter [2].

To improve the aircraft stability, different control strategies, such as gain scheduling, are widely used in the industry [3]. The main idea of this methodology is to design a set of linear controllers for specific operating points over the flight envelope. Gain interpolation is then used between the points to ensure the operation along the entire aircraft envelope. Some of the algorithms used to generate the gain scheduling correspond to linear quadratic regulator (LQR) and eigenstructure assignment among others [2]. Theoretical works applied to the aircraft control are presented in [4, 5] and [6]; therefore, only some of them presents the gains schedule process.

The most important publications are [7] where the comparison of classical LQR is presented (solution of Riccati equation) with Optimal Cooperative control of Ch-47 helicopter; [8] show the results of LQR technique applied to the lateral control of the Boeing 767, later [9] applied the technique on a flexible civil aircraft. Recently, [10] presented the use of advanced flight controls research and development applied to business jet aircraft. [11] propose a methodology to assess the robust stability and robust performance of Automatic Flight Control Systems (AFCS) using gain scheduling and optimization and [12] add the quantum particle swarm optimization (QPSO) to improve the LQR. However, all the mentioned works use the LQR in the time domain employing a considerable number of linear models to guarantee a specific performance and robustness in the overall flight envelope; this process generates several gain scheduling tables.

To improve these methodologies, the  $H_\infty$  strategy was applied by [13], trying to reduce the number of points in the gain schedule process, use an unique structure instead of several gain tables and to increase the operating domain with a lower set of gains. With the same purpose and aiming its industrial implementation, this paper presents an

alternative project, the two degree of freedom (TDOF) controller proposed by [14] to design stability and control augmentation systems.

Some advantages of TDOF controller are its pragmatical design, once it depends only on two parameters (a third one can be added to corrects the steady state error); in comparison with the LQR controllers mentioned above, its project is done in the frequency domain instead of time domain. The feedback gains affects the stability of the system and the pre-filter the response characteristics. The controller exhibits robustness to plant uncertainties and if the sensitivity and complementary sensitivity functions are considered [15], the controller achieves disturbances rejection and noise attenuation [16]. Additionally, the controller has a unique structure (e.g., does not contain tables). The strategy in the frequency domain (solution of Diophantine equation) has been successfully implemented only for the trajectory control problem in a SCARA<sup>1</sup> robot [17].

This paper presents as novelty an alternative practical project in the development of control laws for fly-by-wire aircrafts, adding handling qualities requirements to comply with certification authority's request. The TDOF controller application is made on a business jet aircraft; also it is possible to design it for commercial and cargo aircrafts.

In Sect. 2, the mathematical model is described. Handling qualities criteria are presented in Sect. 3. The main characteristics of the TDOF controller and its algorithm are described in Sect. 4. The design of controller and linear simulations is presented in Sect. 5. The baseline aircraft handling qualities analysis and results are presented in Sect. 6. The results of nonlinear simulations for regulation and tracking maneuvers are presented in Sect. 7. Finally, the conclusions are presented.

## 2 Mathematical modeling

The motion of an aircraft as a rigid body can be described by a set of nonlinear simultaneous differential equations. These equations, representing the translational and rotational motion of the aircraft, can be formulated as state variable (SV) equations expressed as:

$$\dot{x}(t) = f[x(t), u(t)] \quad (1)$$

$$y(t) = h[x(t), u(t)] \quad (2)$$

where  $x(t)$  is the internal state vector,  $\dot{x}$  is the derivative of  $x(t)$  with respect to time,  $u(t)$  is the control vector [in this paper, the control vector is given only by elevator deflection  $\delta_e(t)$ ] and  $y(t)$  is the measured outputs.

<sup>1</sup> Selective Compliance Assembly Robot Arm.

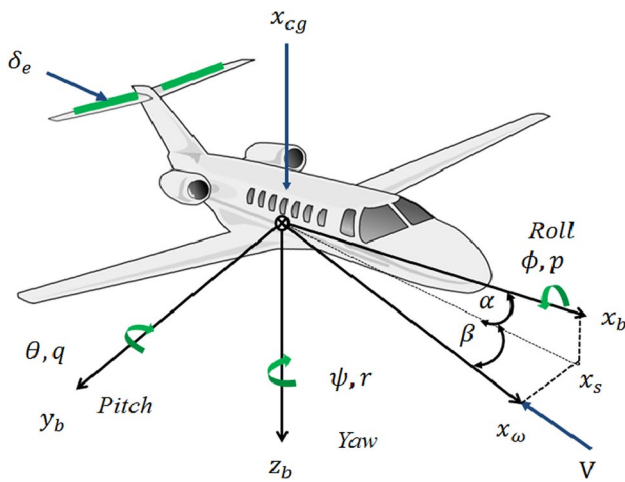


**Fig. 1** Coordinate systems and main aircraft variables

The origin of the body axis system  $(x_b, y_b, z_b)$  illustrated in the Fig. 1<sup>2</sup> is the aircraft center of gravity  $x_{cg}$ . The  $x_b$  axis is directed toward the nose of the aircraft, the  $y_b$  axis toward the right wing, and the  $z_b$  axis toward the bottom of the aircraft. Additionally, Fig. 1 shows the angular velocities roll, pitch and yaw rate  $(p, q, r)$ . The attitude angles  $(\phi, \theta, \psi)$ , angle of attack  $\alpha$  and sideslip angle  $\beta$  are also illustrated; details can be consulted in [2] and [18]. The nonlinear model of the generic business jet aircraft assembled in Matlab/Simulink presented in [19] is considered in this paper.

A common practice in flight controls, when designing and analyzing control systems, is to linearize the aircraft equations around an operating point (trim point). Therefore, nonlinear equations of the aircraft (1)–(2) are linearized for different operating points of its envelope, usually parameterizing by airspeed and altitude.

The longitudinal axis linear models of aircraft, obtained at different operation points to design and analyze the TDOF controller, are represented by standard linear state equation given by

$$\begin{aligned} \dot{x}(t) &= Ax(t) + B\delta_e(t) \\ y(t) &= Cx(t) \end{aligned} \tag{3}$$

where  $A \in \mathcal{R}^{4 \times 4}$  is the state matrix,  $B \in \mathcal{R}^{4 \times 1}$  is the input matrix,  $C \in \mathcal{R}^{1 \times 4}$  is the output matrix and  $x = [V_{TAS} \ \alpha \ \theta]^T$  is the state variable. In this paper, the main interest is the relationship from elevator deflection  $\delta_e(t)$  to pitch rate  $q(t)$ , which transfer function is defined as:

$$G(s) = \frac{q(s)}{\delta_e(s)} \tag{4}$$

<sup>2</sup> Adapted from <http://www.wpclipart.com/transportation/aircraft/jet>

**Table 1** Elevator actuator parameters

Surface	$\omega_n$ [rad/s]	$\zeta$
Elevator	35	0.5

**Table 2** Transport delay of sensors

Signal	$V_{TAS}$ [m/s]	$\theta$ [rad]	$q$ [rad/s]	$\alpha$ [rad]
$\tau$ [ms]	190	26	26	115

### 2.1 Actuator and sensors models

The actuator and sensors models are introduced in the analysis model, only to verify the closed-loop stability and to evaluate the handling qualities.

The actuator model corresponds to a second-order filter. Table 1 presents the adopted values of natural frequency and damping for the actuator.

The sensors dynamics were modelled considering the delays presented in Table 2.

The transfer function of time delay is irrational (it has not  $s$ -polynomial in the numerator and denominator). For this reason, it is necessary to use an approximation in the form of rational transfer function. The approximation used corresponds to 4th order Padé approximation.

### 2.2 Mass, airspeed and center of gravity configurations

The robustness specifications for the aircraft longitudinal dynamics were analyzed considering the flight envelope configurations for mass  $m$ , calibrated airspeed  $V_{CAS}$  and center of gravity along the body  $x$  axis  $x_{cg}$ . Table 3 shows the set of nine models extracted from aircraft envelope, considering three airspeed conditions and an arrangement of five  $x_{cg}$  mass configurations. The main target of the proposed design is to get a unique fixed gain TDOF controller to cover all conditions of Table 3.

## 3 Handling qualities

Three handling qualities (HQ) criteria are used in the design. As suggested in references [13] and [6], the use of the HQ criteria is made in the design verification phase to evaluate good response to a pilot input. From [20], the response of the pilot is evaluated according to the following criteria:

**Table 3** Linear models generated for  $V_{CAS} \times x_{cg}$  envelope

$V_{CAS}$ [knots]	$x_{cg}$ [%]		
93	29	40	47
96	22	29	32
106		32	40
		40	47

- Level 1 satisfactory: Flying qualities clearly adequate for the mission Flight Phase. Desired performance is achievable with minimal pilot compensation.
- Level 2 acceptable: Flying qualities adequate to accomplish the mission Flight Phase, but some increase in pilot workload or degradation in mission effectiveness, or both.
- Level 3 controllable: Flying qualities such that the aircraft can be controlled in the context of the mission Flight Phase, even though pilot workload is excessive or mission effectiveness is inadequate, or both.

**3.1 Modal criteria**

This criterion is related essentially with the damping ratios of aircraft modes: the short period and the phugoid [2].

The slow oscillating mode, known in aviation terms, as phugoid is generally under-damped. It mainly affects the pitch attitude and the true velocity. To reach the flying qualities required for level 1 of a typical HQ criterion such as the Cooper Harper, the phugoid damping ratio shall be greater than 0.04 [20].

A rapid oscillating mode (short period) mostly affects the transient responses in the baseline aircraft angle of attack  $\alpha$ , pitch rate  $q$  and load factor  $Nz$ . To meet the flying qualities required for level 1, then the short period damping ratio shall be greater than 0.4 [20].

**3.2 Bandwidth criterion**

The criterion establishes that a measure of the handling qualities of an aircraft is based on its stability margin when commanded by pilot in a closed loop compensatory pitch attitude tracking task. The maximum frequency that such closed loop tracking can be accomplished without disturbing stability is referred to as bandwidth [21].

The control bandwidth of aircraft is critically important to good handling and the flight control system easily modifies it. The control bandwidth is further complicated by the fact that it varies with the inputs–outputs variables involved. Namely, control and handling difficulties may arise when the bandwidth of an input–output relationship is lower than it should be. For this reason, all input–output bandwidth properties should be consistent and chosen to

**Table 4** Handling qualities requirements

Handling qualities	Level 1	Good level 1
Short period damping $\zeta_{sp}$	$0.4 < \zeta_{sp} < 1.35$	$0.7 < \zeta_{sp} < 1.35$
$\theta$ -Bandwidth	$>1.5$ [rad/s]	$>1.75$ [rad/s]
$\gamma$ -Bandwidth	$>0.6$ [rad/s]	
Phase delay $\tau_p$	$>0.1$ [s]	$>0.09$ [s]
Gain margin	$>6$ [dB]	$>10$ [dB]
Phase margin	$>30$ [°]	$>45$ [°]

lead to good aircraft handling and adequate stability margins. Two measures for that are the pitch attitude and the flight path angle bandwidth criterion (attitude bandwidth versus flight path bandwidth indicate consonance between attitude and flight path response) [22].

From frequency response, the pitch attitude bandwidth is defined as the lower of the pitch attitude gain bandwidth,  $\omega_{BW_{gain}}$ , and the pitch attitude phase bandwidth,  $\omega_{BW_{phase}}$ . Otherwise, the gain bandwidth,  $\omega_{BW_{gain}}$ , is defined by the frequency at which the gain margin is 6 dB; in other words, it is the frequency correspondent to the gain 6 dB higher than the gain when the phase is  $-180^\circ$ . The phase gain bandwidth,  $\omega_{BW_{phase}}$ , is defined by the frequency at which the phase margin is  $45^\circ$ , or this is the frequency at which the phase first passes  $-135^\circ$  (is  $45^\circ$  higher than  $-180^\circ$ ) [23].

**3.3 Phase delay criterion**

In [23], it is established that the roll-off in phase due to a time delay  $\tau$  is a linear function of frequency. It is observed that, at frequencies around and higher than the bandwidth frequency, the curve of the Bode phase response of a high-order function is reasonably well matched by the equivalent phase delay. Consequently, the phase delay based on the baseline aircraft attitude response may be defined by following equation:

$$\tau_p = \frac{\Delta\phi_{2\omega_{180}}}{2\omega_{180}} \frac{\pi}{180} \tag{5}$$

where  $2\omega_{180}$  is twice the neutral stability frequency, i.e., the frequency at  $-180^\circ$  phase, and  $\Delta\phi_{2\omega_{180}}$  is the phase at that frequency.

Table 4 summarizes the handling quality boundaries being considered in the design procedure.

**4 Two degree of freedom controller**

The design of the TDOF, the dominant dynamics is the aircraft. Therefore, the actuator and sensor transfer functions

are not considered in the controller design. The structure of the TDOF controller is presented in Fig. 2.

The baseline aircraft longitudinal axis to be controlled is represented by the minimal, strictly proper rational transfer function given by Eq. (4):

$$G(s) = \frac{c(s)}{a(s)} = \frac{q(s)}{\delta_e(s)} \tag{6}$$

where polynomials  $a(s)$  and  $c(s)$  are co-prime, with degrees  $n$  and  $m$  ( $m < n$ ). The inputs  $d(s)$  and  $\eta(s)$  correspond to aircraft disturbance and sensor noise signal. The polynomials  $h(s)$ ,  $k(s)$  and  $\hat{q}(s)$  of degrees  $n - 1$  are the controller functions.

The closed-loop transfer function from  $r(s)$  to  $q(s)$ , with-out aircraft disturbance  $d(t)$  and sensor noise signal  $\eta(t)$  is

$$\frac{q(s)}{r(s)} = \frac{\kappa c(s)\hat{q}(s)}{a(s)k(s) + c(s)h(s)} = \frac{\kappa c(s)\hat{q}(s)}{\delta(s)} \tag{7}$$

where  $\kappa \in \mathcal{R}$  and  $\delta(s)$  represents the closed-loop polynomial.

The controller guarantees a good output regulation, by positioning per design the roots of  $\delta(s)$  far enough into the left half  $s$  plane. However, the design could increase the system bandwidth sufficiently to produce the baseline aircraft control effort  $\delta_e(t)$  saturation; in our case, the elevator commands cannot exceed the physical design limits. Complementarily, one way of obtaining a desirable output regulation, without requiring an excessive control effort signal, is to design the aircraft longitudinal axis controller by minimizing the LQR performance index, which is

$$J_{LQR} = \int_0^\infty \left\{ \rho(r(t) - q(t))^2 + \delta_e(t)^2 \right\} dt \tag{8}$$

The excessive output excursions and the control effort required to prevent such excursions can be obtained by minimizing the Eq. (8). The adjustable weighting

factor  $\rho \in \mathcal{R}^+$  can be used to obtain appropriate trade-offs between these two conflicting goals. The time solution of (8) corresponds to matrix gains calculated by the Riccati equation and the equivalent solution in the frequency domain is known as spectral factorization [14].

### 4.1 Spectral factorization

Since the polynomials  $a(s)$  and  $c(s)$  have real coefficients, it follows that both:

$$\begin{aligned} a(j\omega)a(-j\omega) &= |a(j\omega)|^2 \geq 0 \\ c(j\omega)c(-j\omega) &= |c(j\omega)|^2 \geq 0 \quad \forall \text{ real } \omega \end{aligned} \tag{9}$$

Therefore, it is possible to define:

$$\Delta(s) = a(s)a(-s) + \rho c(s)c(-s) \tag{10}$$

where  $\Delta(s)$  is an even polynomial given by:

$$\Delta(s) = (-1)^n s^{2n} + \Delta_{2n-2} s^{2n-2} + \dots + \Delta_2 s^2 + \Delta_0 \tag{11}$$

The  $2n$  roots of  $\Delta(s)$  are obtained with  $\rho$  varying from 0 to  $\infty$  and represent a special root locus which is termed as root-square locus, i.e., if  $\lambda_j$  is a root of  $\Delta(s)$ , then  $-\lambda_j$  is also a root of  $\Delta(s)$ . Consequently,  $\Delta(s)$  can be expressed by a spectral factorization as:

$$\Delta(s) = [\Delta(s)]^+ [\Delta(s)]^- = \delta^{F^*}(s) \delta^{F^*}(-s) \tag{12}$$

where  $n$  stable roots of  $[\Delta(s)]^+$  allow to obtain  $\delta^{F^*}(s)$ .

By duality, spectral factorization also can be used to obtain the  $n$  stable roots of  $\delta^{H^*}(s)$ , which is defined as the left half-plane spectral factor of

$$\begin{aligned} \bar{\Delta}(s) &= a(s)a(-s) + \sigma c(s)c(-s) \\ &= [\bar{\Delta}(s)]^+ [\bar{\Delta}(s)]^- \\ &= \delta^{H^*}(s) \delta^{H^*}(-s) \end{aligned} \tag{13}$$

where each choice of  $\sigma \in \mathcal{R}^+$  in Eq. (13) implies a corresponding  $\delta^{H^*}(s)$ ; consequently, the pre-filter  $\hat{q}(s)$  is calculated as function of  $n$  stable roots of  $\delta^{H^*}(s)$ . Then, for

$$k(s) = s^{n-1} + k_{n-2} s^{n-2} + \dots + k_1 s + k_0 \tag{14}$$

and

$$h(s) = h_{n-1} s^{n-1} + \dots + h_1 s + h_0 \tag{15}$$

it is possible to solve the Diophantine equation.

$$a(s)k(s) + c(s)h(s) = \delta^{F^*}(s)\hat{q}(s) \tag{16}$$

Equation (16) can be written as:

$$S\mathcal{V} = \bar{\delta} \tag{17}$$

where

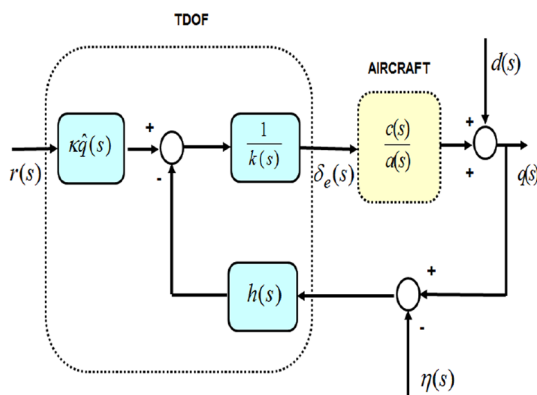


Fig. 2 TDOF controller structure

$$S = \begin{pmatrix} a_0 & 0 & \dots & 0 & c_0 & 0 & \dots & 0 \\ a_1 & a_0 & \dots & 0 & c_1 & c_0 & \dots & 0 \\ \vdots & \vdots & \ddots & \vdots & \vdots & \vdots & \ddots & \vdots \\ a_{n-1} & a_{n-2} & \dots & a_0 & c_{n-1} & c_{n-2} & \dots & c_0 \\ 1 & a_{n-1} & \dots & a_1 & 0 & c_{n-1} & \dots & c_1 \\ 0 & 1 & \dots & a_2 & 0 & 0 & \dots & c_2 \\ \vdots & \vdots & \ddots & \vdots & \vdots & \vdots & \ddots & \vdots \\ 0 & 0 & \dots & 1 & 0 & 0 & \dots & 0 \end{pmatrix}$$

$$\mathcal{V} = (k_0 \ k_1 \ \dots \ k_{n-1} \ h_0 \ h_1 \ \dots \ h_{n-1})^T$$

$$\bar{\delta} = \begin{pmatrix} (\delta^{F^*}(s)\hat{q}(s))_0 \\ (\delta^{F^*}(s)\hat{q}(s))_1 \\ \vdots \\ (\delta^{F^*}(s)\hat{q}(s))_{2n-2} \\ (\delta^{F^*}(s)\hat{q}(s))_{2n-1} \end{pmatrix}$$

From Eq. (17), the real coefficients of gains  $h(s)$  and  $k(s)$  are obtained.

### 5 Design of TDOF controller

The linear model used to design the TDOF controller corresponds to aircraft take-off condition at (altitude = 2000 ft,  $V_{CAS} = 93$  knots,  $x_{cg} = 0.47$  and mass = 11,500 Kg). The matrices  $A$ ,  $B$  and  $C$  obtained at this condition for longitudinal axis are given by

$$A = \begin{pmatrix} -0.0533 & 5.3316 & -0.0770 & -9.8060 \\ -0.0083 & -0.6399 & 0.9736 & 0.0000 \\ 0.0033 & -0.4201 & -0.5483 & 0 \\ 0 & 0 & 1.0000 & 0 \end{pmatrix} \tag{18}$$

$$B = (0.0193 \ -0.0545 \ -1.2061 \ 0)^T$$

$$C = (0 \ 0 \ 1 \ 0)$$

According Eq. (3), the transfer function  $\frac{q(s)}{\delta_e(s)}$  is given by:

$$\frac{-1.206s^3 - 0.8132s^2 - 0.09385s + 2.828e^{-018}}{s^4 + 1.242s^3 + 0.8675s^2 + 0.08011s + 0.05443} \tag{19}$$

**Table 5** Eigenvalues of design linear model

Eigenvalues	$\zeta$
$2.52e^{-3} + 2.60e^{-1}j$	$-9.70e^{-3}$
$2.52e^{-3} - 2.60e^{-1}j$	$-9.70e^{-3}$
$-6.23e^{-1} + 6.46e^{-1}j$	$6.94e^{-1}$
$-6.23e^{-1} - 6.46e^{-1}j$	$6.94e^{-1}$

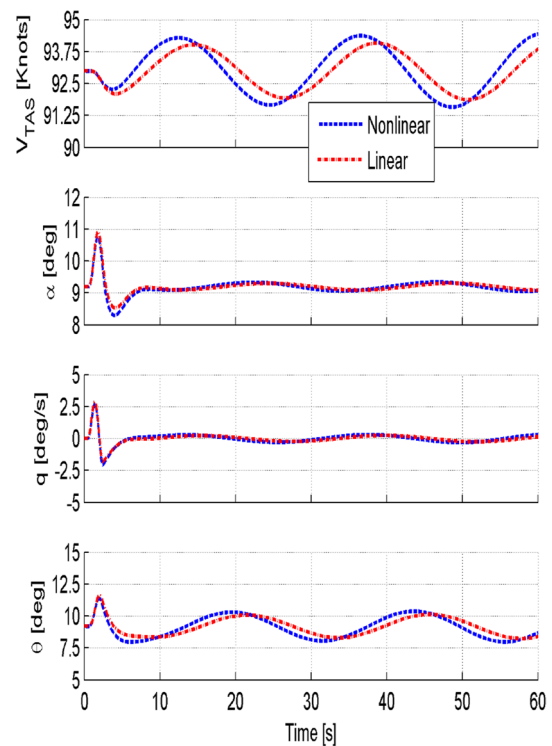


**Fig. 3** Linear and nonlinear response to  $\delta_e$  doublet

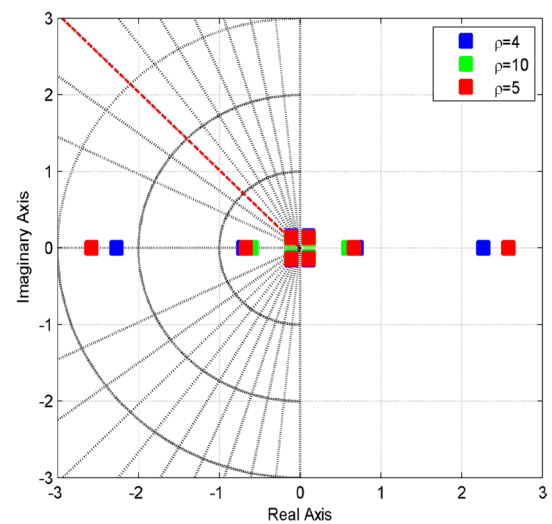


**Fig. 4** A Root-Square locus plot for  $\Delta(s)$

where the eigenvalues and damping are presented in Table 5.

To verify the accuracy of the linear model design, the response of aircraft to  $\delta_e$  doublet was compared with non-linear response at the same condition. Figure 3 illustrates the open loop response of both models, where it is possible to verify that the linear model is representative of aircraft dynamics at the selected operation condition and suitable

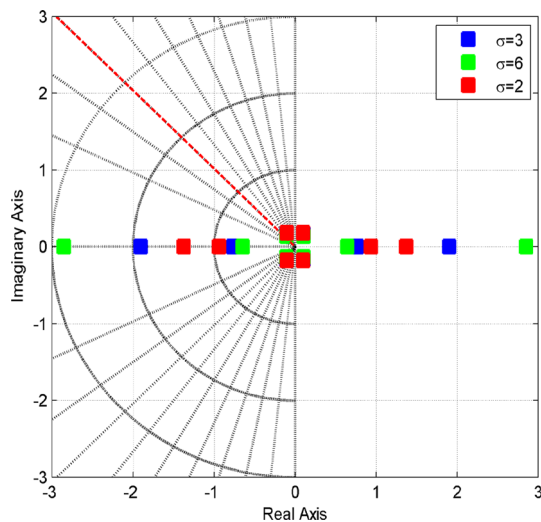


**Fig. 5** A Root-Square locus plot for  $\bar{\Delta}(s)$

**Table 6** The values of root-square locus

$\rho = 5$	$\sigma = 2$
-2.5792	-1.3718
2.5792	1.3718
0.6669	-0.9381
-0.6669	0.9381
$0.1073 + 0.1419j$	$0.0989 + 0.1803j$
$0.1073 - 0.1419j$	$0.0989 - 0.1803j$
$-0.1073 + 0.1419j$	$-0.0989 + 0.1803j$
$-0.1073 - 0.1419j$	$-0.0989 - 0.1803j$

**Table 7** TDOF controller gains

$\hat{q}(s)$	$h(s)$	$k(s)$
$1.0000s^3$	$-1.8254s^3$	$1.0000s^3$
$2.4088s^2$	$-4.6310s^2$	$2.4260s^2$
$1.5153s$	$-3.1631s$	$1.3493s$
$0.1270$	$-0.6271$	$0.1270$

to the design purpose; also it is possible to confirm that the long period dynamics is unstable.

### 5.1 Design results

Figure 4 allows verifying the root-square locus from Eq. (10) considering three values of weighting factor  $\rho$ .

Figure 5 allows verifying the root-square locus from Eq. (13) considering three values of weighting factor  $\sigma$ .

To comply with the requirements given in the Table 4, the values of root-square locus for weighting factors  $\rho = 5$  and  $\sigma = 2$  are selected. They are detailed in Table 6.

The weighting factor  $\rho$  makes possible fulfilling with the closed loop stability requirements (fast pole location without actuator saturation) through the calculation of  $\Delta(s)$  to obtain the polynomial  $\delta^{F^*}(s)$  as:

$$\delta^{F^*}(s) = s^4 + 3.4606s^3 + 2.4481s^2 + 0.4717s + 0.0544 \tag{20}$$

at the same time, the weighting factor  $\sigma$  helps to fulfilling with handling qualities requirements (values greater than 2 do not meet the requested) through the calculation of  $\bar{\Delta}(s)$  to obtain the polynomial  $\delta^{H^*}(s)$  as:

$$\delta^{H^*}(s) = s^4 + 2.5077s^3 + 1.7859s^2 + 0.3522s + 0.0543 \tag{21}$$

Considering Eq. (21), the pre-filter  $\hat{q}(s)$  is calculated as:

$$\hat{q}(s) = (s + 0.9381)(s + 1.3718)(s + \text{real}(0.0989 - 0.1803j)) \tag{22}$$

Finally, using the Diophantine Eq. (17), the 3rd order polynomials  $h(s)$  and  $k(s)$  presented in Table 7 are obtained.

Figure 6 illustrates the simulation results obtained, for all nine model conditions, using a pulse input signal, the gains of Table 7 and a selected  $\kappa = -1$ . In these results, it is evident from the steady-state error.

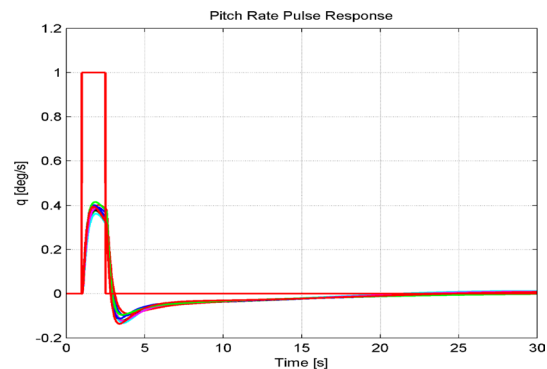


**Fig. 6** Pulse input response  $\kappa = -1$

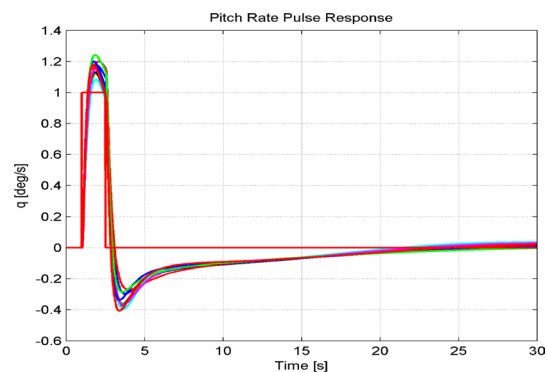


**Fig. 7** Pulse input response  $\kappa = -2.99$

Figure 7 illustrates again, the simulation results obtained using a pulse input signal, the gains of Table 7 and a selected  $\kappa = -2.99$ .

Results presented in the Figs. 6 and 7 allow to verify that the  $\kappa$  gain was tuned considering the mean value in steady state of all model configurations. Therefore, gains were selected based on the frequency, damping and steady-state error around zero.

### 6 Handling qualities analysis

The closed loop poles of all linear model conditions of Table 3 are represented by the filled squares illustrated in Fig. 8. From this, results can be verified that requested

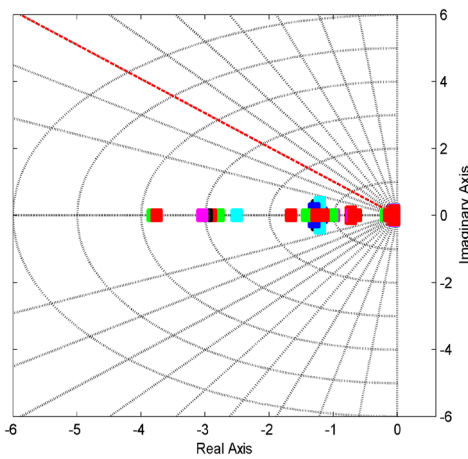


Fig. 8 Close loop poles

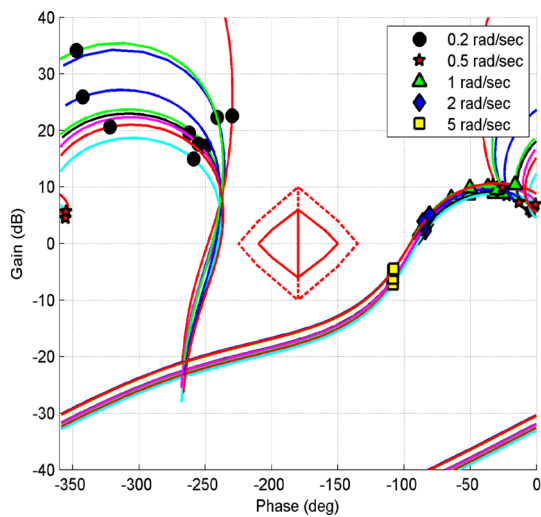


Fig. 9 Magnitude versus phase for elevator

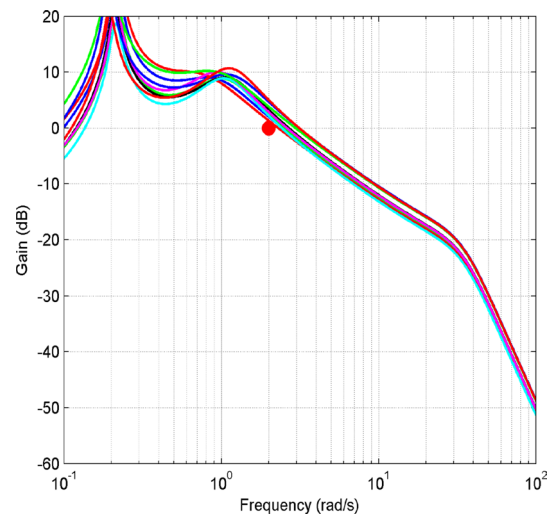


Fig. 10 Gain versus frequency for elevator

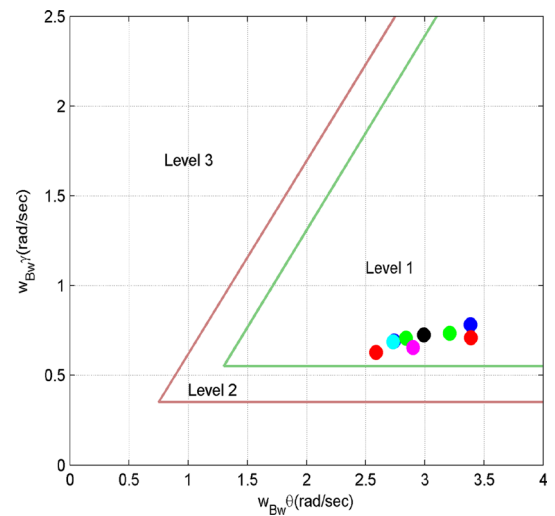


Fig. 11  $\gamma$  – bandwidth versus  $\theta$  – bandwidth

short period damping requirements are reached, in this case greater or equal than 0.7.

Figure 9 illustrates the Nichols plots for linear models, where the horizontal and vertical axis of rhomboid represents the phase and gain margin boundaries, respectively. From these, results can be verified that the requirements for gain and phase margin requested in Table 4 are satisfied, that is the phase margin is greater than  $45^\circ$  and gain margin is greater than 10 dB.

Figure 10 illustrates the gain versus frequency response of elevator. This result shows that the crossover frequency for all cases is around 2 radians per second, which is considered appropriate for this design.

Figure 11 shows the results for  $\gamma$  bandwidth versus  $\theta$  bandwidth, where the filled points represent each analyzed



case. The limits presented in this figure were obtained from [13] and [21] and they are applicable for a business jet aircraft.

The results accomplish the requirements for the bandwidth criteria presented in Table 4, because  $\theta$ -bandwidth is greater than 2 radians by second and the  $\gamma$ -bandwidth is greater than 0.6 radians by second.

Figure 12 shows the results for phase delay criteria versus  $\theta$ -bandwidth.

The results accomplish the requirements for the criterion presented in Table 4, because  $\theta$ -bandwidth is greater than 2 radians by second and the phase delay  $\tau_p$  is lower than 0.09 seconds.

### 7 Nonlinear simulation results

This section presents the results of nonlinear simulations; two cases are considered, the first one is regulation with and without TDOF controller and the second is tracking to

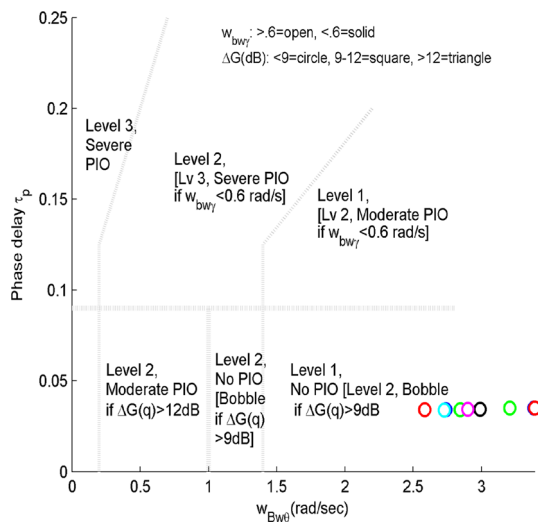


Fig. 12 Phase delay versus  $\theta$ -bandwidth

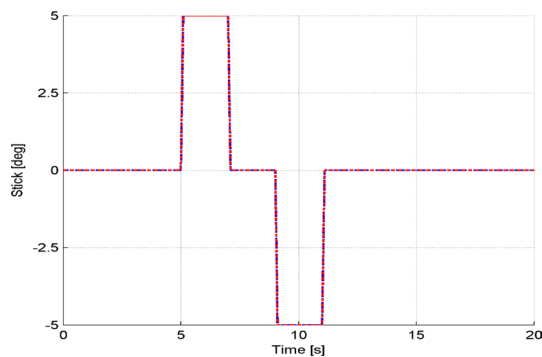


Fig. 13 Longitudinal stick input

compare with gain schedule technique (with interpolated tables).

### 7.1 Regulation

Figure 13 shows the longitudinal input of nonlinear simulation until 20 s.

The nonlinear simulation results for the aircraft in cruise condition, at altitude = 5000 ft,  $V_{CAS} = 142$  knots,  $x_{cg} = 0.32$  and mass = 13,500 Kg, are illustrated in Fig. 14.

From the results, it can be observed and verified that the augmented aircraft response (with TDOF controller) when

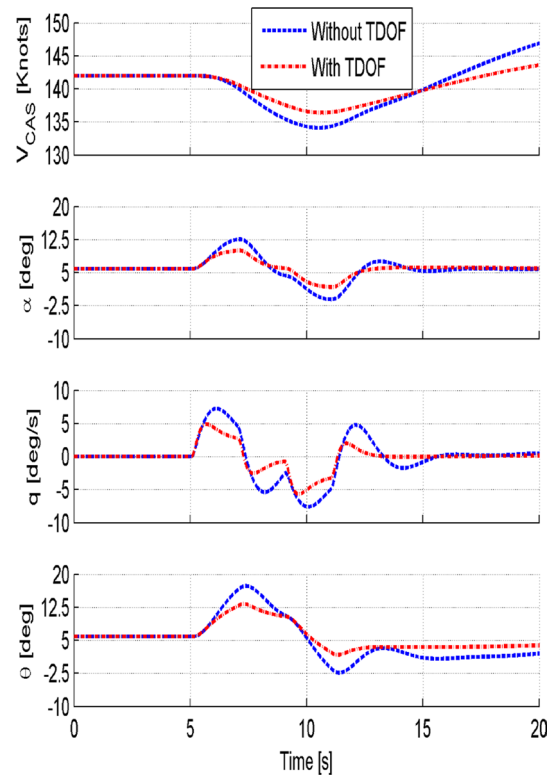


Fig. 14 Nonlinear simulation results

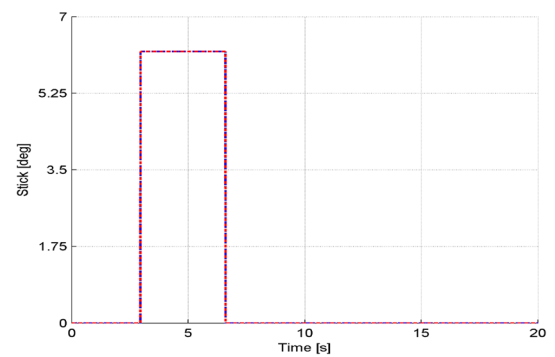
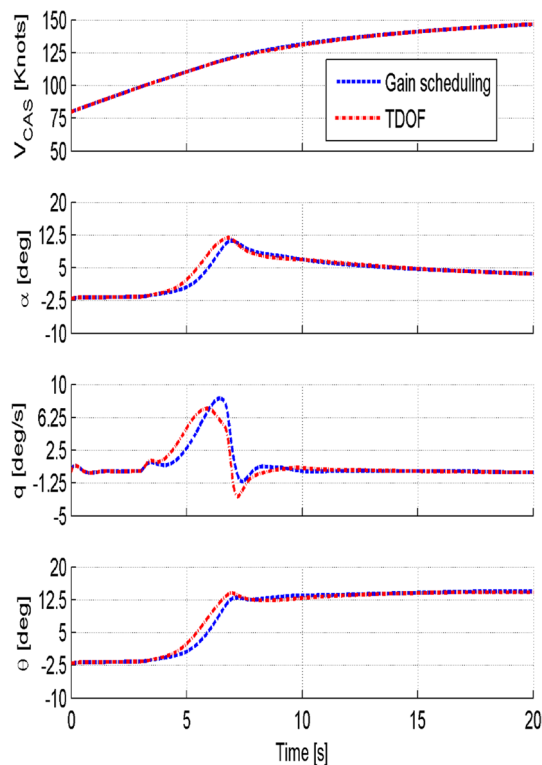


Fig. 15 Longitudinal stick input



**Fig. 16** Comparison results TDOF Vs. Gain Scheduling

compared with the non-augmented aircraft (without TDOF controller) does not present oscillations, therefore as waited achieves a significantly better response.

## 7.2 Tracking

Figure 15 shows the longitudinal input of nonlinear simulation until 20 s. The positive input is given between 3 and 6.5 s; the input has been set equal to 0 between 6 and 20 s.

The nonlinear simulation results for the aircraft in take-off condition, at altitude = 2000 ft,  $V_{CAS} = 80$  knots,  $x_{cg} = 0.30$  and weight = 14,000 Kg, are illustrated in Fig. 16.

From the results, it can be seen that the aircraft with TDOF controller presents a faster response to reach  $12.5^\circ$  of  $\theta$  when compared with the gain schedule controller (interpolated gain tables are illustrated in the Fig. 17).

## 8 Conclusions

This paper presents the project of Stability and Control Augmentation System with two TDOF controller. To design the controller, LQR technique in the frequency domain, via spectral factorization, is used and handling qualities requirements are included in the design criteria.

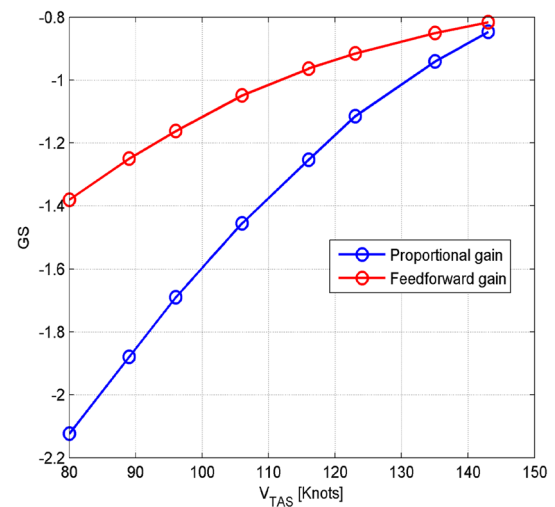


**Fig. 17** Gain scheduling breakpoints

The design uses a linear model. The weighting factors  $\rho$  and  $\sigma$  were selected using the root-square locus. The gain  $\kappa$  was tuned considering zero steady error for a pulse input response. The handling qualities analysis was performed to guarantee compliance with certification authority's requests.

The robustness to uncertainties was verified considering the controller at models with different configuration of mass, center of gravity and airspeed. Also, simulation with nonlinear model was performed showing the performance of TDOF controller in regulation and tracking maneuvers.

The design of TDOF controller was demonstrated to be a straightforward approach. Moreover, it represents an practical alternative solution to gain schedule technique. In this case, it is possible to use a unique fixed structure instead of interpolated tables. From the point view of certification, it can be asserted that verification process would be simplified using this project.

**Acknowledgments** The authors would like to thank to Daniel Siqueira for HQ's templates, to seniors engineers Paulo Donato and Michel McSharry for the text reviews and finally to EMBRAER and ITA for financial support.

## References

- Holzappel F, Heller M, Weingartner M, Sachs G, da Costa O (2006) Development of control laws for the simulation of a new transport aircraft. In: 25th International Congress of the Aeronautical Sciences
- Stevens BL, Lewis FL (2003) Aircraft control and simulation, 2nd Edn. Wiley, New York, USA
- Leithead W (1999) Survey of gain scheduling: analysis and design. Int J Control 73:1001–1025

4. Nair VG, Dileep MV, George VI (2012) Aircraft yaw control system using lqr and fuzzy logic controller. *Int J Comput Appl* 9(45):25–30
5. Akyazi O, Usta MA, Akpınar AS (2012) A self-tuning fuzzy logic controller for aircraft roll control system. *Int J Control Sci Eng* 6(2):181–188 doi: [10.5923/j.control.20120206.06](https://doi.org/10.5923/j.control.20120206.06)
6. Saussié D, Akhrif O, Saydy L (2005) Longitudinal flight control design with handling quality requirements. Département de génie électrique École Polytechnique de Montréal et École de Technologie Supérieure, Janvier
7. Townsend BK (1986) The application of quadratic optimal cooperative control synthesis to a CH-47 Helicopter, 1st edn. NASA Technical Memorandum 88353
8. Gangsaas D, Bruce K R, Blight JD, Ly UL (1986) Application of modern synthesis to aircraft control: three casestudies. *IEEE Trans Autom Control*:995–1014
9. Aouf N, Boulet B, Botez R (2002) A gain scheduling approach for a flexible aircraft. *Proceeding of the American Control Conference*, pp 4439–4442
10. Gangsaas D, Hodgkinson J, Harden C (2008) Multidisciplinary control law design and flight test demonstration on a business jet. *AIAA Guidance, Navigation and Control Conference and Exhibit*, pp 1–25
11. da Silva ASF, Paiva HM, Kienitz KH (2011) A methodology to assess robust stability and robust performance of automatic flight control systems. *Rev Bras Controle Autom* 22(5):429–440
12. Hassani K, Lee WS (2014) Optimal tuning of linear quadratic regulators using quantum particle swarm optimization. *Proceedings of the International Conference of Control, Dynamics and Robotics*, pp 1–8
13. Siqueira D, Moreira FJO, Paglione P (2007) Robust flight control design supported by flying qualities analysis. *AIAA Guidance, Navigation and Control Conference*, South Carolina, pp 1–8
14. Wolovich WA (1994) Automatic control systems: basic analysis and design, 2nd edn. The Oxford Series in Electrical and Computer Engineering Series. Saunders College Pub, New York
15. Zhou K, Doyle JC (1997) Essentials of robust control, 1st edn. Prentice Hall, New Jersey
16. Vargas FJT, de Pieri ER, Castelan EB (2004) Identification and friction compensation for an industrial robot using two degrees of freedom controllers. In: *ICARCV, IEEE*, pp 1146–1151
17. Vargas FJT (2004) Experimental implementation of robust and intelligent controllers in trajectory control of industrial scara robot. In: KaGnicheM (ed) *Student Forum, IFIP 18 th World Computer Congress-Student Forum, 22–27 August 2004, Toulouse, France*, Kluwer, pp 415–428
18. Duke EL, Antoniewicz RF, Krambeer KD (1988) Derivation and definition of a linear aircraft model, 1st edn. NASA Reference Publication 1207, USA
19. Stengel RF (2004) *Flight dynamics*, 1st edn. Princeton University Press, Princeton, NJ
20. MIL-F-8785C (1980) *Flying qualities of piloted airplanes*, Military Norm
21. Tischler MB (1996) *Advances in aircraft flight control*, 1st edn. Taylor and Francis Publishers, London
22. AGARD/NATO (1991) *Handling qualities of unstable highly augmented aircraft*. Advisory report, Research and Technology, North Atlantic Treaty Organization
23. David KA (1996) Comparison of the control anticipation parameter and the bandwidth criterion during the landing task. In: *Master degree Thesis*, Air Force Institute of Technology